Mass-balance modelling of Gangotri glacier

A. AGRAWAL[1], R. J. THAYYEN[2] & A. P. DIMRI[1]*

[1]*School of Environmental Sciences, Jawaharlal Nehru University, New Delhi, India*

[2]*National Institute of Hydrology, Roorkee, Uttarakhand, India*

**Correspondence: apdimri@hotmail.com*

Abstract: The sensitivity of glacier mass balance (MB) in response to climatic perturbations has made it an important parameter of study from hydrological, climatological and glaciological point of view. To monitor the health of any glacier system, long-term MB observations are required. These observations among Himalayan glaciers are not available consistently and large glaciers are not often monitored for mass balance due to logistical challenges. One such glacier is the Gangotri, situated in the western Himalaya. In the present study an attempt is made to model the MB over the Gangotri glacier, the biggest glacier in the Ganga basin and also the point of origin of the River Ganges. The mass balance of the Gangotri glacier is estimated during the time period 1985–2014 using two different methods: ice-flow velocity; and energy balance modelling using regional model (REMO) outputs and *in situ* automatic weather station (AWS) data. The geodetic method is used for the nearby Dokriani glacier, where field-based MB measurements are available. MB of Gangotri glacier estimated for 2001–14 using the ice-flow velocity method is -0.92 ± 0.36 m w.e. a^{-1}; for 2006–07, MB using AWS and Tropical Rainfall Monitoring Mission (TRMM) data with the energy balance modelling approach is -0.82 m w.e. a^{-1}; and for 1985–2005, MB using REMO data with the energy balance modelling approach is -0.98 ± 0.23 m w.e. a^{-1}. Using the surface velocity method, it is estimated that the glacier lost 9% of its volume during the period 2001–14. The glacier vacated an area of 0.152 km^2 from the snout region, and retreated by 200 m in the last 14 years. MB values estimated for the Gangotri glacier from different methodologies are remarkably close, suggesting them to be suitable methods of MB estimation. TRMM, High Asia Refined (HAR-10) and Asian Precipitation Highly Resolved Observational Data Integration Towards Evaluation of water resources (APHRODITE) data are used to estimate the precipitation over the glacier. The study suggests that the glacier-wide estimation of weather parameters needs to be improved for more accurate estimation of glacier mass balance.

Supplementary material: The snow-covered area, for months Jan-Dec, obtained for Gangotri glacier using Landsat data and NDSI (normalized differencing snow index) for year 2014 is available at https://doi.org/10.6084/m9.figshare.c.3888091

The study of glaciers is of immense significance for understanding and predicting global environmental change. They play a very important role in the regulation of Earth's energy budget. Whenever there is a climatic perturbation glaciers respond by gaining or losing mass, eventually leading to a change in their length, area and elevation. Change in glaciers causes change in the regional hydrology and therefore downstream flow regimes (Thayyen & Gergan 2010). So far, mass-balance (MB) studies in the Himalaya have been concentrated among a few medium- and small-sized glaciers (Dobhal *et al.* 2008; Bolch *et al.* 2011). However, in the Himalayan catchments where downstream flows are dominated by the monsoon during the peak glacier melt period of July and August (Thayyen & Gergan 2010), contributions from these small glaciers have a limited influence. Larger glaciers such as Gangotri glacier have a decisive impact on the downstream flow regimes of the headwater reach of the River Ganga. The mean annual summer runoff from the Gangotri glacier catchment, including 258.56 km^2 of Gangotri glacier system, is about 522 million cubic metres (MCM; Kumar *et al.* 2002). In comparison to this, average summer runoff generated from the nearby Dokriani glacier catchment (15.7 km^2) with 7 km^2 glacier cover is merely 54 MCM (Thayyen & Gergan 2010). Being the largest glacier in the Ganga headwater region as well as the source of the River Ganga, the MB perturbations of Gangroti are of immense scientific interest. There are a number of varying views regarding the response of the Gangotri glacier to the changing climate of the region. Some suggest that the Gangotri glacier has retreated fast during the past three decades (IPCC 2007), while others suggest that the retreat of the glacier has slowed down during the recent past (Kumar *et al.* 2008; Raina 2009). There are also viewpoints which caution against linking the present climate response of glaciers with that of glacier recession of the large 30 km long glaciers such as Gangotri (Thayyen 2008). The uncertainty over the response

From: Pant, N. C., Ravindra, R., Srivastava, D. & Thompson, L. G. (eds) *The Himalayan Cryosphere: Past and Present*. Geological Society, London, Special Publications, **462**, https://doi.org/10.1144/SP462.1

of Gangotri glacier to the present and immediate past climate can only be removed by evaluating the glacier MB. However, considering the steep challenges associated with carrying out glaciological MB studies over the Gangotri glacier, MB modelling is found to be the only viable option.

Being one of the largest glaciers in the Himalaya, a number of studies have already been carried out on Gangotri glacier. Some of the studies are on runoff measurement, meteorology and suspended load (Singh *et al.* 2005, 2008, 2010; Haritashya *et al.* 2006). The discharge of the Gangotri glacier system at the catchment outlet, covering 556 km^2 of glacier and non-glacier area, ranged over 10–250 m^3 s^{-1} for the period 2005–06 for the months May–October (Singh *et al.* 2010). Different studies have reported different retreating rates of the glacier during the past decades: 819 ± 14 m or *c.* 20 m a^{-1} for 1965–06 (Bhambri *et al.* 2012); and 1519 m or *c.* 22 m a^{-1} for 1935–04 (Kumar *et al.* 2008). The meteorological data for 2001–08 suggests several reasons for retreat: reduction in fresh snowfall amount during winter; increase in rainfall amount during summer; decrease in snowfall days; increase in rainfall days; or the rising trend of average temperature in the Gangotri sub-basin (Negi *et al.* 2012). The glacier flow velocity is found to vary from 28.1 ± 2.3 m a^{-1} at the lower elevations to 48.1 ± 2.3 m a^{-1} at the higher elevations (Saraswat *et al.* 2013). A number of recent studies have tried to estimate the volume of the Gangotri glacier: 23.2 ± 4.2 km^3 (Gantayat *et al.* 2014); 21.559 km^3 (Haq *et al.* 2014); 20.6 km^3 (Glacier bed topography (Glabtop2); Frey et al. (2014)); and 21.1 km^3 (Huss and Farinotti (HF)-model; Frey *et al.* 2014). Haq *et al.* (2013) estimated the average mass balance of Gangotri glacier during 2001–09 as −0.289 m a^{-1} using the geodetic method. Kargel *et al.* (2011) reported a stabilized terminus and thinning of Gangotri glacier by about 5 m based on the analysis of ASTER digital elevation models from 2001 and 2006 images. MB for nearby glaciers – Dokriani (−0.32 m w.e. a^{-1} during 1993–00; Dobhal *et al.* 2008) and Chorabari (−0.73 m w. e. a^{-1} during 2003–10; Dobhal *et al.* 2013) – have been reported from field studies. In the present study, MB of the Gangotri glacier is estimated using two different methods: energy balance modelling and the ice-flow velocity method. MB of the Dokriani glacier has also been estimated by the geodetic method and compared with the field MB value.

Study area

The Gangotri glacier (Fig. 1a) is located in the Uttarkashi district of Uttarakhand and lies within longitude 79° 04′ 41″–79° 16′ 4″ E and latitude 30° 44′–30° 56′ N (Kumar *et al.* 2008). The glacier has immense religious significance and is a vital source of freshwater supply for the people living downstream. The glacier is 30 km long and originates from Chaukhamba massif and flows towards Gaumukh (snout of Gangotri). The River Bhagirathi

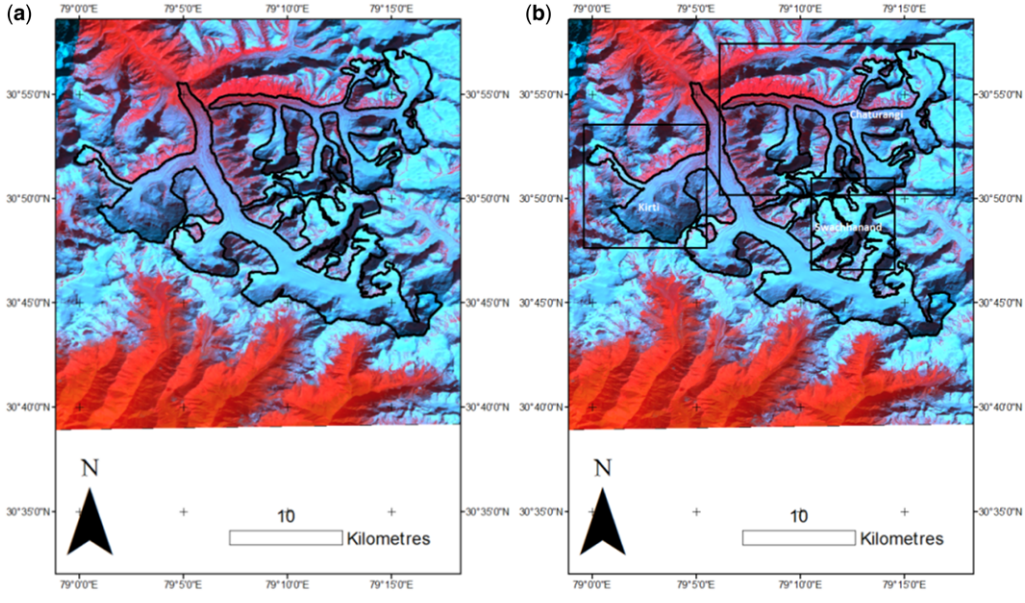

Fig. 1. (**a**) Outline of Gangotri glacier on Landsat image acquired on 23 October 2002 and (**b**) Chaturangi, Kirti and Swachhanand tributaries of the glacier shown on Gangotri glacier.

originates from the glacier and meets Alaknanda at Devprayag to form the Ganga River. Gangotri lies in the rain shadow zone of the monsoon and the average mean summer precipitation at Bhojwasa (3792 m a.s.l) is 250 mm w.e. Significant precipitation in the form of snow occurs in the region from the Indian winter monsoon (Dimri 2012). The altitude gradients of both winter and summer monsoon precipitation are available for the region. Seasonal melting in this region takes place during May–October (Saraswat *et al.* 2013). The Gangotri group of glaciers has six tributary valley glaciers (Fig. 1b) feeding from either side of the trunk glacier (Gantayat *et al.* 2014). Its surface elevation ranges over 4200–7000 m a.s.l. It is 30.2 km long and has a mean width of 1.5 km with a surface area of 140 km^2 and volume of 23.2 ± 4.2 km^3; the glacier is 540 m thick in the upper reaches and 50–60 m near the snout region (Gantayat *et al.* 2014). The major part of the glacier's ablation area is debris covered (Singh *et al.* 2010), which adds to the complexity of the glacier by affecting its albedo and melting patterns. Important features of the glacier and the studies carried out on the glacier are summarized in Tables 1 and 2, respectively.

Lying to the SW of the Gangotri glacier system in the Garwhal Himalaya, Dokriani glacier (30° 50′–30° 52′ N and 78° 47′–78° 50′ E; Fig. 2) is 5.5 km long and covers an area of 7 km^2. It flows from 6632 to 3890 m a.s.l. One-third of the ablation zone of the glacier is covered with thick supraglacial debris (Dobhal *et al.* 2008).

Meteorological data

AWS

Data from three automatic weather stations (AWS) located at Bhojwasa (3792 m a.s.l., 30° 55′ N, 79° E), Nandanvan (4500 m a.s.l., 30° 54′ 18″ N, 79° 06′ 08″ E) and Kalandikhal (5948 m a.s.l., 30° 44′ 18″ N, 79° 11′ 54″ E) provided daily air temperature, air pressure, snow depth, relative humidity, wind speed, and shortwave incoming and outgoing radiation for the time period May 2006–April 2007. The data are generated through the Department of Science and Technology (DST) supported project by the Snow and Avalanche Study Establishment (SASE). Precipitation and temperature data from the nearby Dingad catchment for years 1994, 1998–01 and 2003–04 from the weather stations located in Tela (2540 m a.s.l., 30° 51′ 26″ N, 78° 40′ 39″ E), Gujjar hut (3483 m a.s.l., 30° 50′ 50″ N, 78° 45′ 00″ E) and base camp of Dokriani glacier (3763 m a.s.l., 30° 52′00″ N, 78° 47′ 00″ E) (Thayyen & Gergan 2010) are also used to test the robustness of the meteorological information derived from the models.

Table 1. *Features of Gangotri glacier*

Features	Gangotri glacier
Range (m a.s.l.)	4200–7000
Slope (degree)	5.15
Orientation	NW
Debris cover (%)	29
Latitude (°N)	30.45–30.55
Longitude (°E)	79.0–79.2

TRMM

TRMM (Tropical Rainfall Measuring Mission) is a research satellite launched by NASA and Japan Aerospace Exploration Agency (JAXA) on 27 November 1997 from Tanegashima, Japan. It is designed to improve the understanding of distribution and variability of precipitation within the tropics as part of the water cycle in the current climate system. In the present study, TRMM precipitation data from 2000 onwards is used. The resolution of the data is 0.25° × 0.25°.

REMO

REgional MOdel (REMO) data from the COrdinated Regional Climate Downscaling Experiment (CORDEX) was downloaded from http://esg-cccr.tropmet.res.in/esgf-web-fe/. Monthly longwave upwelling radiation, longwave downwelling radiation, shortwave upwelling radiation, shortwave downwelling radiation, sensible heat flux, latent heat flux and precipitation were downloaded for the time period 1985–2005.

APHRODITE

The daily APHRODITE (Asian Precipitation Highly Resolved Observational Data Integration Towards Evaluation of water resources) data of resolution 0.25° × 0.25° for the time period 1994–2007 was downloaded from http://www.chikyu.ac.jp/precip/ (Yatagai *et al.* 2012). APHRODITE's daily gridded precipitation is a long-term (1951 onwards) continental-scale daily product. It contains a dense network of daily rain-gauge data for Asia, including Himalayas, south and SE Asia and mountainous areas in the Middle East.

HAR

The High Asia Refined (HAR) atmospheric dataset is generated using the atmospheric model WRF (Weather Research and Forecast) version 3.3.1. The model is driven by final analysis data from the global forecasting system with additional sea-surface

Table 2. *Literature review of Gangotri glacier*

Parameter	Gangotri	Year/period	Reference
Length (km)	30		Kumar *et al.* (2008), Singh *et al.* (2010), Gantayat *et al.* (2014)
Width (km)	0.5–2.5		Kumar *et al.* (2008)
	0.2–2.35		Singh *et al.* (2010)
	1.5		Gantayat *et al.* (2014)
Area (km^2)	Shrank by 4.4 ± 2.7; frontal recession 0.38 ± 0.03	1968–2006	Bhambri *et al.* (2011)
	0.41 ± 0.03 loss at the snout	1965–2006	Bhambri *et al.* (2012)
	258.56 with Rakhtvarn and Meru	1965–2006	Kumar *et al.* (2008)
	140 (without Rakhtvaran, Meru and Chaturangi)	1965–2006	Gantayat *et al.* (2014)
Thickness (m)	540 in the upper reaches to 50–60 near the snout by ice-flow velocity method	2009–2010	Gantayat *et al.* (2014)
	145 by GlabTop2	2012	Frey *et al.* (2014)
Volume (km^3)	23.24.2	2009–2010	Gantayat *et al.* (2014)
	39.18	2009–2010	Kumar *et al.* (2008)
	21.6	2009–2010	Haq *et al.* (2014)
	20.6 (by GlabTop2)	2009–2010	Frey *et al.* (2014)
MB ($m\ a^{-1}$)	−0.289 by geodetic method (ASTER DEM)	2001–2009	Haq *et al.* (2013)
Velocity ($m\ a^{-1}$)	14–85 in the accumulation region to 20–30 near the snout	2009–2010	Gantayat *et al.* (2014)
Retreat (m)	700	1976–2009	Ambinakudige (2010)
	819 ± 14	1965–2006	Bhambri *et al.* (2012)
	1519	1935–2004	Kumar *et al.* (2008)
Discharge ($m^3\ s^{-1}$)	10–250	2005–2006 (May–October)	Singh *et al.* (2010)

temperature input. HAR provides gridded data for fields such as temperature, precipitation and wind at 30 km resolution for Central Asia and 10 km resolution for the Tibetan Plateau and surroundings. HAR provides data on an hourly basis starting in 2001. It is being used as a tool for studying atmosphere-related processes on the Tibetan Plateau, where other types of observations are scarce. In this study HAR-10 precipitation and temperature data are downloaded (http://www.klima.tu-berlin.de/index.php?show=forschung_asien_tibet_har&lan=en) for the time periods 2001–07 and 2000–14.

Area and elevation data

For Dokriani glacier, the toposheet of scale 1:10 000 was generated by the Survey of India through a special mapping project in 1995.

Landsat

Landsat 8 is an American Earth observatory satellite which was launched on 11 February 2013. Landsat 8 Operational Land Imager (OLI) and Thermal Infrared Sensor (TIRS) images consist of nine spectral bands with a spatial resolution of 30 m for bands 1–7 and 9. New band 1 is for coastal and aerosol studies, and new band 9 is for cirrus cloud detection. The resolution for band 8 (panchromatic) is 15 m. Thermal bands 10 and 11 are for providing surface temperatures, collected at 100 m resolution.

Cloud-free Landsat8 images were downloaded from Earth explorer (http://earthexplorer.usgs.gov/), acquired on: 21 May, 4 and 30 June, 21 October, 20 and 21 November and 7 December 2013; and 28 March, 13 August and 14 September 2014.

The Landsat 7 images were also downloaded from Earth explorer, acquired on: 20 October 2001; 23 October 2002; and 23 July 2015. The datasets used in the study are summarized in Table 3.

A number of Landsat 5 images were also downloaded for the study, acquired on: 3 November 2009; 14 February, 27 March, 28 April, 17 May and 15 June 2010; 9 January, 17 February, 21 March and 24 October 2011; and 24 December 2012.

Cartosat-1

Cartosat-1 satellite, designed for cartography applications, was launched by the Department of Space

Latitude										
30.56										
30.54						G	G			
30.52			Dokriani			G	G			
30.5			Dokriani			G	G			
30.48						G	G			
30.46						G	G			
30.42										
30.4										
Longitude	78	78.2	78.4	78.6	78.8	79	79.2	79.4	79.6	79.8

G=Gangotri

Fig. 2. Location of Gangotri and Dokriani glaciers.

(DOS), Government of India on 5 May 2005. The satellite provides high-resolution near-instantaneous stereo data. It has a spatial resolution of 2.5 m and radiometric resolution of 10-bit quantization. The high-resolution stereo data can be used to generate high-quality digital elevation models (DEMs). Cartosat-1 DEMs, acquired in 2008, for Gangotri and Dokriani glaciers (28° N, 78° E and) were downloaded from http://bhuvan3.nrsc.gov.in/bhuvan/bhuvannew/bhuvan2d.php.

Thickness and volume estimation for years 2001 and 2014

The volume of the Gangotri glacier was estimated using the ice-flow velocity method. Landsat images acquired on 20 November 2013 and 28 March 2014 are atmospherically and geometrically corrected. The COSI-corr module of ENVI software is used to calculate surface velocities. Velocities are computed using sub-pixel correlation between pixels of band 8 of the above two Landsat images. Subpixel correlation is performed using a sliding window of 32 × 32 pixels with a step size of 4 pixels. The resulting image is triple layered (north/south, east/west, SNR). Regions with SNR < 0.8 are removed from the image obtained. Total surface displacement is computed, and the velocity field is found by dividing the magnitude of surface displacement by the difference in time between when the two images were acquired. The velocity estimated is used to compute pointwise thickness of ice using the equation (Gantayat *et al.* 2014):

$$H = \sqrt[4]{\frac{1.5U}{Af^3(\rho g \sin\alpha)^3}} \quad (1)$$

where U is the surface velocity of ice; A is the creep parameter (3.24×10^{-24} $Pa^{-3}s^{-1}$ as used by Gantayat *et al.* 2014 for Gangotri glacier), assuming a temperate glacier; ρ is the density of ice (900 kg m^{-3}, Oerlemans 2001; Cooper *et al.* 2007); g is the acceleration due to gravity (*c.* 9.81 m s^{-2}); f is shape factor with an average value of *c.* 0.8 (Haeberli & Hoelzle 1995; Linsbauer *et al.* 2012); H is ice thickness (m); and α is surface slope. With the exponent $n = 3$, the glacier ice is assumed to follow Glen's flow rule. With identical inclination angles of the surface and bedrock, the glacier is assumed to be a parallel-sided slab. Ice is assumed to deform under self-weight as an incompressible, non-linear viscous material. Using thickness calculated from Equation (1), the Triangulated Irregular Network (TIN) is prepared for the glaciers. The 'polygon volume' function is used to compute the volume of the glacier. Similarly, the images acquired on 20 October 2001 and 23 October 2002 are analysed to estimate volume of the glacier for the year 2001.

Table 3. *Datasets used in the study*

Date	Sensor	Mission	Path/Row	Pixel resolution (m)
20.10.2001	TM	Landsat 7	145/39	30
23.10.2002	TM	Landsat 7	145/39	30
20.11.2013	OLI	Landsat 8 (band 8)	146/38	15
28.03.2014	OLI	Landsat 8 (band 8)	146/38	15
14.09.2014	OLI	Landsat 8	145/39	30
09.01.2011	TM	Landsat 5	146/39	30
17.02.2011	TM	Landsat 5	146/39	30
27.03.2010	TM	Landsat 5	146/39	30
28.04.2010	TM	Landsat 5	146/39	30
17.05.2011	TM	Landsat 5	146/39	30
15.06.2010	TM	Landsat 5	146/39	30
23.07.2015	ETM+	Landsat 7	146/39	30
13.08.2014	OLI	Landsat 8	145/39	30
14.09.2014	TM	Landsat 5	146/39	30
24.10.2011	TM	Landsat 5	146/39	30
03.11.2009	TM	Landsat 5	146/39	30
24.12.2012	TM	Landsat 5	146/39	30
16.01.2011	TM	Landsat 5	146	39
14.02.2010	TM	Landsat 5	146	39
21.03.2011	TM	Landsat 5	146	39
31.05.2013	OLI	Landsat 8	146	39
04.06.2013	OLI	Landsat 8	146	39
30.06.2013	OLI	Landsat 8	146	39
21.10.2013	OLI	Landsat 8	146	38
21.11.2013	OLI	Landsat 8	146	39
07.12.2013	OLI	Landsat 8	146	38
2006–2008		Cartosat DEM-1	30 N, 79 E	2.5 m
2000–2014		TRMM		0.25° × 0.25°
Model data				
1985–2005		CORDEX, REMO		0.44° × 0.44°
1994–2007		APHRODITE		0.25° × 0.25°
2000–2007		HAR-10		10 km × 10 km
Field data				
1995		Toposheet		1:10 000
1992–2000		MB		Point data
2006–2007		AWS		Point data

Mass-balance estimation

Geodetic method

The long-term MB changes are best estimated by the geodetic method (Zemp *et al.* 2009). The method involves the measurement of change in the glacier surface elevation for two distinct periods (Kaser *et al.* 2003). In this work, the DEM constructed using the Survey of India toposheet specially mapped in 1:10 000 scale in 1994 for Dokriani glacier is subtracted from the Cartosat-1 DEM 2008. The DEM difference yielded the MB for the Dokriani glacier for the period 1994–2008.

Ice-flow velocity method

The mean mass balance of Gangotri glacier is estimated from the difference in the volumes estimated from the ice-flow velocity method for the years 2001 and 2014. Volume loss of a glacier multiplied by the specific density of ice and divided by the surface area (S) of the glacier provides the MB of the glacier. In this study, MB (b) is expressed in units of m w.e. a^{-1}. The density of ice is taken as 900 kg m^{-3} (Oerlemans 2001). MB is calculated via:

$$b = \frac{\Delta V}{S} \times 0.9. \quad (2)$$

Energy balance modelling

Point energy balance modelling. Energy balance modelling was performed using AWS and TRMM/APHRODITE/HAR-10 data for the time period 2006–07, and REMO data for the time

period 1985–2005. Point mass balance can be computed via:

$$b = \text{Accumulation} - \text{Melt} \tag{3}$$

where melt is defined (Hock 2005):

$$\text{Melt} = \frac{Q_\text{m}}{\rho_\text{w} L_\text{f}} \quad \text{(m w.e.)} \tag{4}$$

where Q_m is melt energy; L_f is latent heat of fusion (334 kJ kg^{-1}); and ρ_w is the density of water (1000 kg m^{-3}).

Melt or ablation at a point is calculated from the net energy flux Q_m as calculated below:

$$Q_\text{m} = \Delta Q = Q_\text{ns} + Q_\text{nl} + Q_\text{l} + Q_\text{s} + Q_\text{g} + Q_\text{p} \tag{5}$$

where Q_ns is net shortwave radiation; Q_nl is net longwave radiation; Q_l is latent heat flux; Q_s is sensible heat flux; Q_g is sub-surface heat flux; and Q_p is advected heat from rainwater falling on snow. All terms have the units W m^{-2} (Oerlemans 2001; Hock 2005), and are defined further in the following.

Net shortwave radiation flux.

$$Q_\text{ns} = SWR\downarrow - SWR\uparrow \tag{6}$$

where $SWR\downarrow$ is incoming shortwave radiation flux and $SWR\uparrow$ is outgoing shortwave radiation flux.

Net longwave radiation flux. Incoming longwave radiation is emitted by atmospheric components (vapour, aerosols, clouds) as a function of their temperature. Outgoing longwave radiation is emitted from the glacier or snow surface as a function of its temperature and the properties of the surface. Net longwave radiation is calculated (Oerlemans 2001):

$$Q_\text{nl} = LW\downarrow - LW\uparrow \tag{7}$$

where $LW\downarrow$ is downwelling longwave radiation flux and $LW\uparrow$ is upwelling longwave radiation flux. The downwelling longwave radiation is dependent on the vertical distribution of temperature and vapours in the atmosphere, and the optical properties of clouds if present. It is estimated via the following equation:

$$LW\downarrow = \varepsilon_\text{m} \sigma T_\text{a}^4 \tag{8}$$

where T_a is air temperature; ε_m is atmospheric emissivity; and σ is the Stefan–Boltzmann constant. Atmospheric emissivity ε_m is calculated using the approach suggested by Prata (1996) based on the amount of humidity in the air:

$$\varepsilon_\text{m} = 1 - (1 + w)\exp\left[-(1.2 + 3.0w)^{1/2}\right] \tag{9}$$

where the precipitable water content w (g cm^{-2}) is calculated from an empirical function of vapour pressure e_a (h Pa) and air temperature T_a (K) at 2 m height from the glacier surface:

$$w = 46.5\,(e_\text{a}/T_\text{a}). \tag{10}$$

Vapour pressure e_a (Pa) used in the estimation of precipitable water content is computed using the following equation:

$$e_\text{a} = R_\text{h} \exp(26.23 - 5416/T_\text{a}) \tag{11}$$

where R_h is relative humidity (R_h = 1.0 for saturated air).

Upwelling longwave radiation is computed using the Stefan–Boltzmann law assuming the snow/ice surface is a nearly perfect black body (Hock 2005):

$$LW\uparrow = \varepsilon_\text{s} \sigma T_\text{s}^4 \tag{12}$$

where σ is the Stefan–Boltzmann constant (5.67×10^{-8} W m^{-2} K^{-4}); T_s is the radiative temperature of the surface (K); and ε_s is surface emissivity. The surface emissivity of snow/ice surface is assumed to be unity (Bintanja & van den Broeke 1994). For the computation of net longwave radiation flux, it is assumed in this study that there are no clouds.

Sensible heat flux. Sensible heat flux (SHF) is the heat transfer between the surface and air mass when there is a difference in temperature between them. It depends on the temperature difference between atmosphere and snow pack surface, wind speed, surface roughness and the stability of the air. SHF (W m^{-2}) is computed using the following equation:

$$\text{SHF} = \left(C_\text{p} \frac{\rho_0}{P_0}\right) K_\text{n} P u (T_\text{a} - T_\text{s}) \tag{13}$$

where

$$K_\text{n} = \frac{k^2}{[\log(z_\text{a}/z_0)]^2} \tag{14}$$

where C_p is the specific heat of air (1005 J kg^{-1} K^{-1}); ρ_0 is density of air (1.29 kg m^{-3}) at the standard atmospheric pressure P_0 (1.013×10^5 Pa); K_n is a dimensionless transfer coefficient; P is the mean atmospheric pressure (Pa) at the measuring site; u and T_a are the measured wind speed (m s^{-1})

and air temperature (K); k is von Karman's constant (0.41); z_a is sensor height (m); and z_0 is the aerodynamic roughness length with a value of 0.001 m adopted for the ice surface.

Latent heat flux.

$$\mathrm{LHF} = L_v\left(\frac{0.623\rho_0}{P_0}\right)K_n u(e_a - e_s) \qquad (15)$$

where L_v is latent heat of vaporization; e_a is the vapour pressure at height z_a above glacier surface; and e_s is the saturation vapour pressure at the glacier surface.

The methodology described in this section is applied to compute the point MB from the available AWS data. MB is also computed by the energy balance modelling approach using REMO data. Variables downloaded are used as input in Equation (5) for the computation of melt energy, and Equation (4) is used to compute the melt. Precipitation downloaded and computed melt are used to estimate MB.

The incompatibility of the grid scale and the glacier scale is the key source of error in the use of Regional Climate Model (RCMs) for glacier studies. In the case of the Gangotri glacier, the grid from which REMO data is extracted has 65% glacierized area and 35% non-glacierized area, and Gangotri glacier covers 6% area of this grid (Fig. 3). The data generated for this grid therefore closely reflect the glacier processes. However, in the case of Dokriani glacier grid, only 8% of the grid area is glacierized and Dokriani glacier covers only 2.3% area of this grid; a larger error in the estimate is therefore expected.

Energy balance modelling using temperature lapse rate. The entire glacier is divided into 29 bands, with each band at a gap of 100 m elevation. Temperatures from Bhojwasa, Khalindikhal and Nandanvan AWS stations are used to find monthly average lapse rates for Khalindikhal–Nandanvan and Nandanvan–Bhojwasa. The lapse rates computed are used to estimate the temperatures for all 29 bands of the glacier. The averages of these temperatures are taken to find the monthly average temperatures over the glacier. The average monthly temperature computed is used for the computation of incoming longwave radiation and sensible heat flux for the glacier.

Computing the incoming longwave radiation and sensible heat flux using the above method and computing the outgoing longwave radiation, latent heat flux and shortwave radiation according to the approach described in 'Point energy balance modelling', the mass balance is computed for the glacier using the available AWS and TRMM/APHRODITE/HAR-10 data.

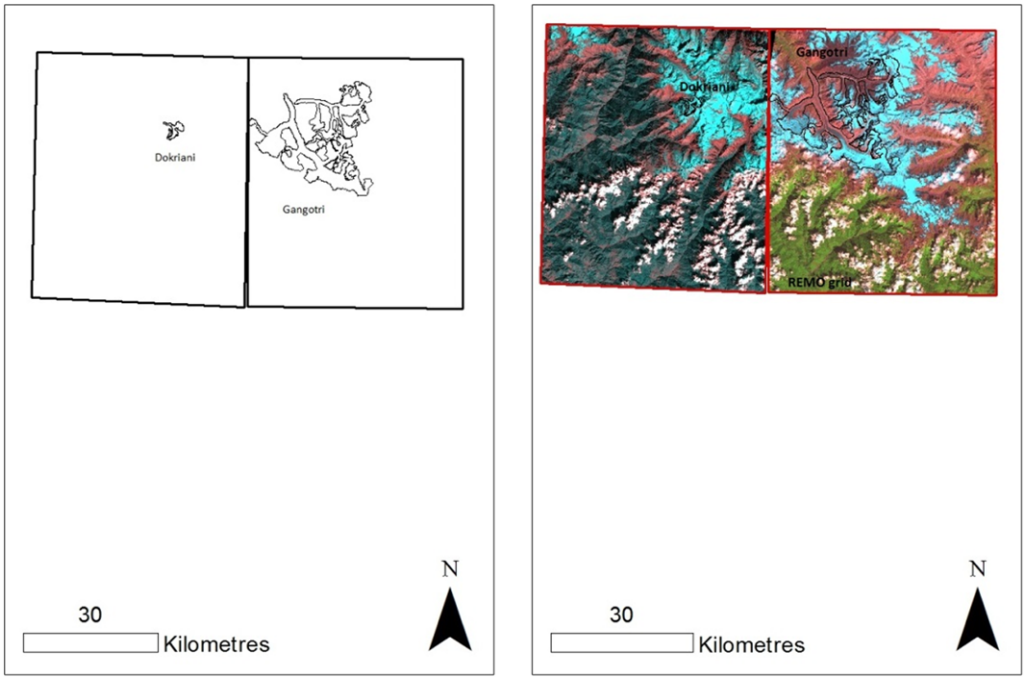

Fig. 3. Gangotri and Dokriani glaciers lying within REMO grid.

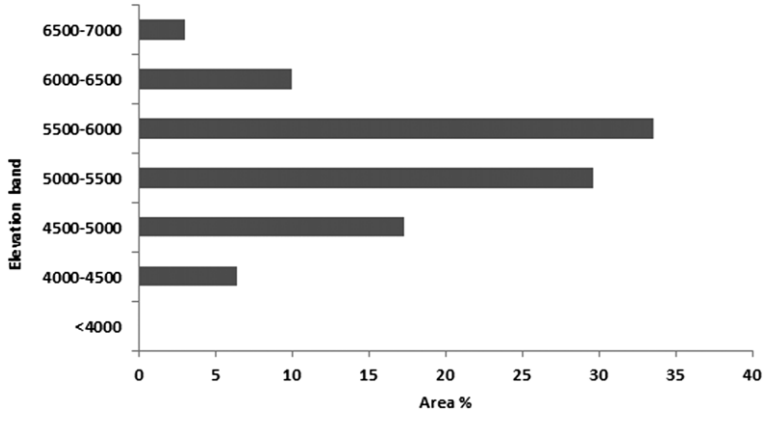

Fig. 4. Hypsometric curve for Gangotri glacier.

Energy balance modelling using Temperature Lapse rate (TLR) and albedo parameterization. Albedo is calculated using the expressions given by Brock *et al.* (2000) and data from the snow-covered region (supplementary material) obtained for Gangotri glacier using Landsat data and NDSI (normalized differencing snow index). According to Brock *et al.* (2000), the albedo of deep snow cover ($\alpha_{ds} >$ 0.5 cm w.e.) and shallow snow cover ($\alpha_{ss} <$ 0.5 cm w.e.) can be calculated using the following equations:

$$\alpha_{ss} = 0.713 - 0.112 \log T_a$$

$$\alpha_{ds} = \alpha_u + 0.422 e^{(-0.058 T_a)} \quad \text{where } \alpha_u = 0.641.$$

SWR is computed for different elevation bands of the glacier using albedo parameterization and hypsometric curve (Fig. 4) for every month. LW ↓ is also calculated using the temperatures computed for all elevation bands of the glacier. LW ↑, SHF and LHF, described in 'Point energy balance modelling', are added to the net SWR and LW ↓. Hypsometric curve and the energy balance obtained are used to compute the total melt from the glacier. TRMM/APHRODITE/HAR-10 precipitation data are added to the computed melt, yielding the mean mass balance for the glacier.

Uncertainty analysis

Different datasets from ground, satellite and climate models at different resolutions have been used in this study. Errors in mass balance results are due to systematic errors inherent in the data, resolution of data and suitability of the methodology used for the calculations. To assess the quality of the results, uncertainties must be computed. Uncertainties in the calculated area, thickness and volume are estimated and discussed in the following sections.

Area estimation

The perimeter of the glacier is estimated on ArcGIS platform. The perimeter is multiplied by half of the resolution of the pixel of the dataset used for area estimation. This gives an estimate of the error in

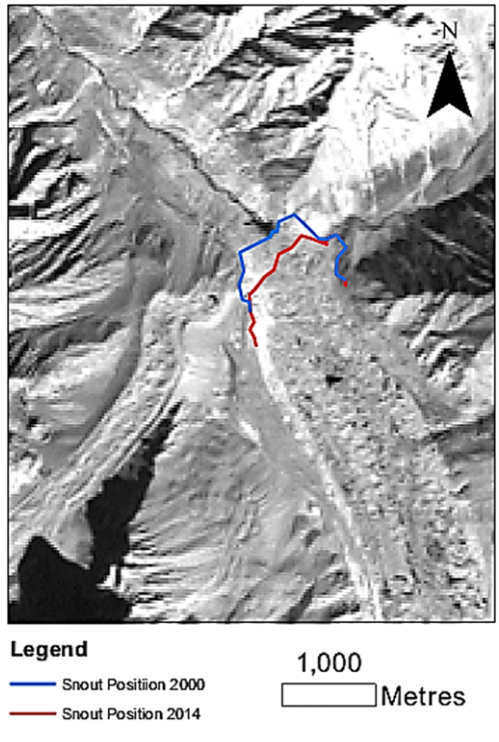

Fig. 5. Change in the snout position from 2000 (top line) to 2014 (bottom line) shown on greyscale Landsat image acquired on 1 October 2000.

area, dS. This value is divided by the actual estimated area to obtain dS/S.

Thickness estimation

Ice thickness is estimated using Equation (1). The uncertainty in thickness is estimated as

$$\frac{\mathrm{d}H}{H} = \frac{1}{4}\left(\frac{\mathrm{d}U}{U} + \frac{\mathrm{d}A}{A} + \frac{3\mathrm{d}f}{f} + \frac{3\mathrm{d}\rho}{\rho} + \frac{3\mathrm{d}g}{g} + \frac{3\mathrm{d}(\sin\alpha)}{\sin\alpha}\right). \tag{16}$$

The value of dU is taken as 3.5 m a^{-1} (Gantayat *et al.* 2014). Uncertainty in the velocity dU/U computed using satellite data becomes *c.* 4.5%. From Gantayat *et al.* (2014), dA/A is taken as 0.26 and df and dρ are set to 0.1 and 90 kg m^{-3}, respectively. Vertical accuracy for the SRTM DEM used is ±20 m (Berthier *et al.* 2007). Average thickness of the glacier is 250 m. The term d(sin α)/sin α therefore becomes $\sqrt{2} \times 20/250$, that is, 0.11. Uncertainty in g is taken as zero. All the above terms together are used to compute dH/H. Equation (16) is a better version of Equation (4) from Gantayat *et al.* (2014), as uncertainties are always added.

Volume estimation

The volume of a glacier is the multiplication of its average thickness by its area. The error estimates in volume are therefore

$$\frac{\mathrm{d}V}{V} = \frac{\mathrm{d}H}{H} + \frac{\mathrm{d}S}{S}. \tag{17}$$

Mass balance estimation

Uncertainty in MB can be calculated as follows:

$$b = (V_2 - V_1) \times \frac{\rho}{S} \tag{18}$$

$$b = (S_2H_2 - S_1H_1)\frac{\rho}{S} \approx (H_2 - H_1)\rho \tag{19}$$

$$b = \rho\left(\sqrt[4]{\frac{1.5U_2}{Af^3(\rho g \sin\alpha_2)^3}}\right) - \rho\left(\sqrt[4]{\frac{1.5U_1}{Af^3(\rho g \sin\alpha_1)^3}}\right) \tag{20}$$

$$\log b = \log\left[\left(\frac{1.5}{A(fg\rho)^3}\right)^{0.25}\left(\frac{u_2^{0.25}}{(\sin\alpha_2)^{0.75}} - \frac{u_1^{0.25}}{(\sin\alpha_1)^{0.75}}\right)\right] + \log\rho \tag{21}$$

Uncertainty in MB can be approximated as:

$$\frac{\mathrm{d}b}{b} \approx \frac{\mathrm{d}H}{H} + \frac{\mathrm{d}\rho}{\rho}. \tag{22}$$

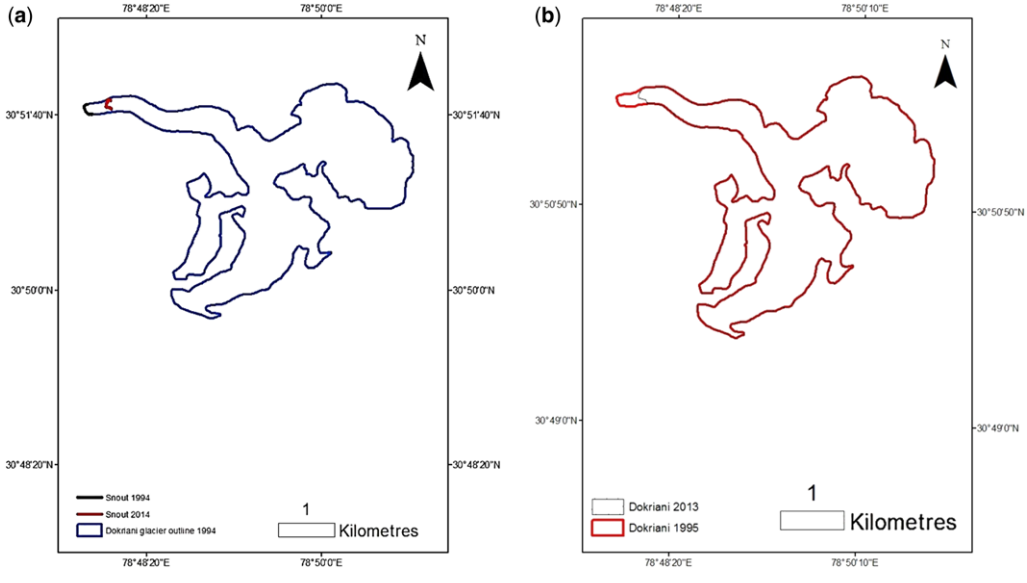

Fig. 6. (**a**) Snout retreat of Dokriani glacier and (**b**) area vacated by Dokriani from the front.

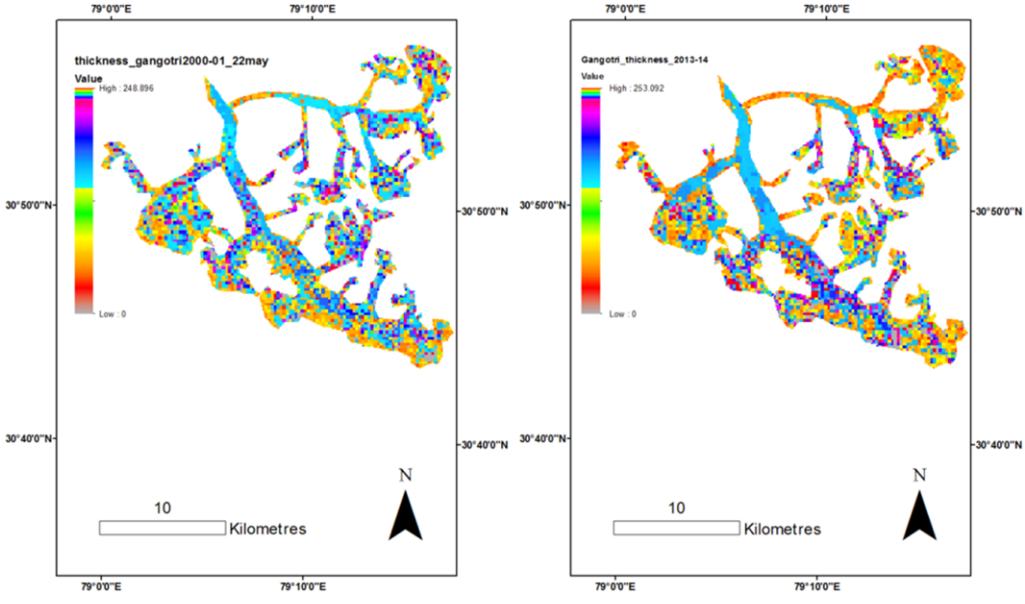

Fig. 7. Thickness profiles of the glacier in years 2001 and 2014.

Results and discussion

Area

The change in area of the Gangotri glacier has been discussed in detail in earlier studies. The study conducted by Bhambri *et al.* (2011) reported that Gangotri glacier shrank by 4.4 ± 2.7 km^2 (0.11 ± 0.07 km^2 a^{-1}) between 1968 and 2006. Other studies, for example Kumar *et al.* (2009), reported that the glacier area reduced by 15.5 km^2 (*c.* 0.51 km^2 a^{-1}) between 1976 and 2006. Bhambri *et al.* (2012) further suggested that the main reason for the discrepancy could be that the terminus of this glacier is debris covered, which obscures snout retreat. Interpretation of debris cover, shadow area and seasonal snow on the coarse satellite images and topographic maps used are also known to be major challenges in glacier studies.

To compute mass balance, the area of the glacier is taken to be 140 km^2 from Gantayat *et al.* (2014). The glacier has vacated an area of 0.6 km^2 (0.023 km^2 a^{-1}) from the snout region and retreated by 1150 m (44.2 m a^{-1}) during the time period 1985–2014. This is close to the value 0.41 ± 0.03 km^2 (0.1 km^2 a^{-1}) loss at the snout from 1968 to 2006 reported by Bhambri *et al.* (2012). The glacier has vacated an area of 0.152 km^2 from the snout region, and retreated a distance of 200 m in the last 14 years (Fig. 5).

The area of Dokriani glacier was 7.02 km^2 in 1995, and 7 km^2 in 2007 (Dobhal & Mehta 2010). In the present study it is observed that the glacier has vacated an area of 0.08 km^2 from the snout during the period 1995–2013 (Fig. 6).

Thickness

Thickness profiles of the glacier calculated by the surface velocity method for the years 2001 and 2014 are estimated to vary over the ranges 35–500 m and 35–450 m, respectively (Fig. 7). These results are comparable with the results reported in different studies (540 m in the upper

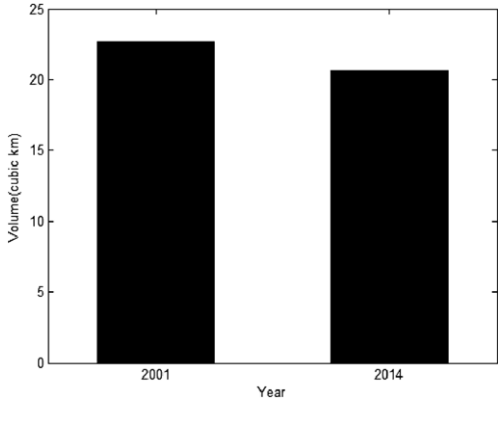

Fig. 8. Volume of Gangotri glacier in 2000 and 2014.

reaches to 50–60 m near the snout for the time period 2009–10; Gantayat *et al.* 2014) and average thickness of 145 m (2012, GlabTop2, Frey *et al.* 2014). From the thickness profiles of the glacier in years 2000 and 2014 (Fig. 7) it is evident that the two tributaries of the glacier, Kirti Bamak (on the left bank of the glacier, 7 km long, peak at 6940 m a.s.l.) and Swachhanand Bamak (on the right bank of the glacier, 7 km long, peak at 6190 m a.s.l.), are thinning at the icefall region close to the confluence point; they may become separated from the trunk glacier if the present recessional trend continues in the future. The Chaturangi glacier, the longest tributary of Gangotri glacier, has already separated from the main glacier trunk.

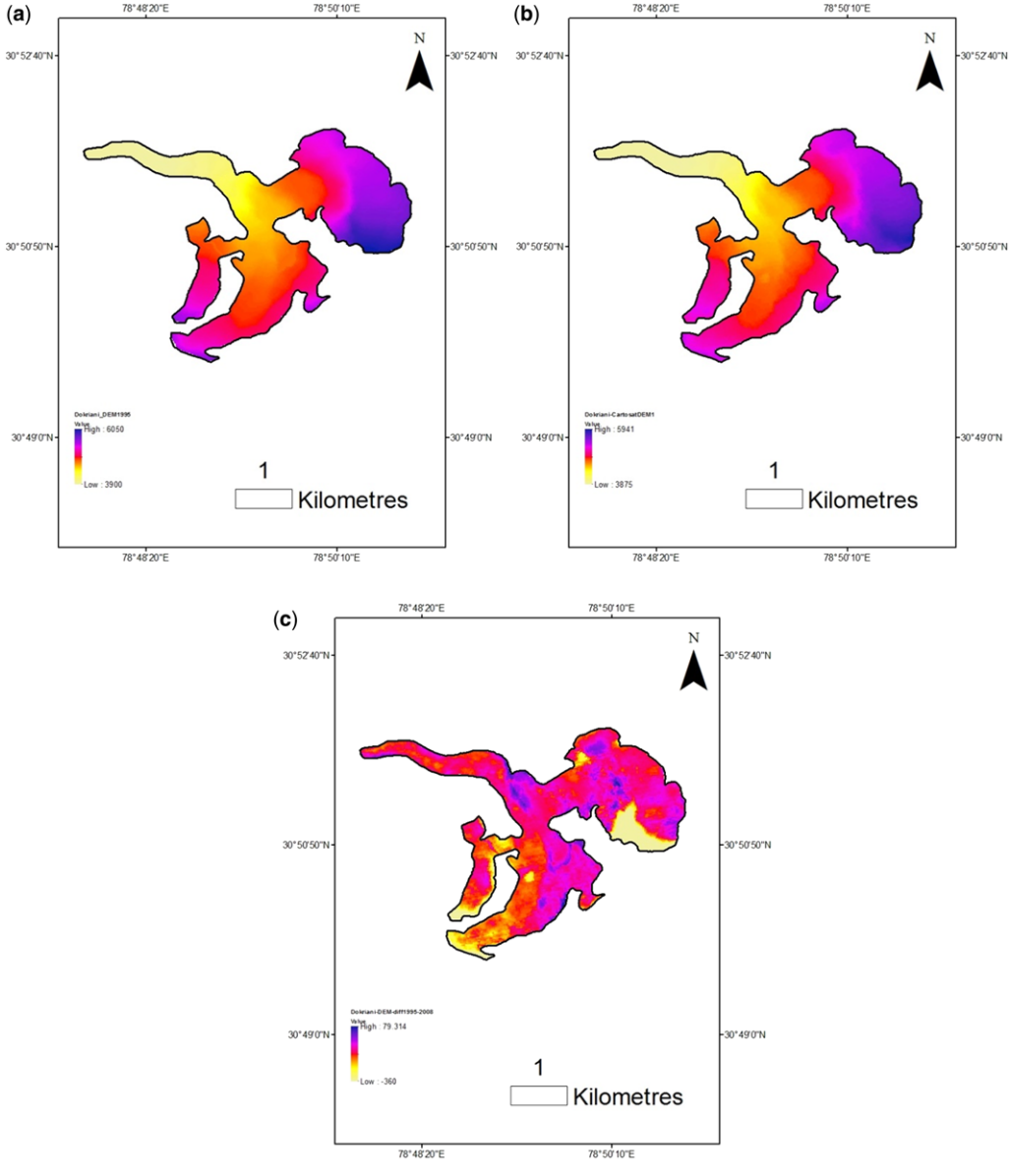

Fig. 9. DEM of Dokriani glacier (**a**) generated using 1995 SOI toposheet and (**b**) extracted from Cartosat DEM-1 (2008). (**c**) Difference between DEMs in (a) and (b).

Volume and mass balance

The volume of the Gangotri glacier for the years 2001 and 2014 is estimated to be 22.70 ± 7.1 km^3 and 20.64 ± 6.4 km^3, respectively (Fig. 8), as calculated by the ice-velocity method. The volumes estimated are close to the reported values: 23.24 km^3 for the time period 2009–10 (ice-flow velocity method; Gantayat *et al.* 2014); 21.6 km^3 for the year 2010 (artificial neural network; Haq *et al.* 2014); and 20.6 km^3 (2012, GlabTop2, Frey *et al.* 2014). None of the previous studies reported a change in volume of Gangotri glacier using the ice-flow velocity method.

The loss of volume of *c.* 2 km^3 in 14 years yields a MB of Gangotri glacier of −0.92 m w.e. a^{-1}. The MB of Dokriani glacier is computed using geodetic method (Fig. 9), and is found to be −0.27 m w.e. a^{-1} for 1995–2008. This is close to the average annual MB reported by Dobhal *et al.* (2008) for the time period 1992–2000, that is, −0.32 m w.e. a^{-1}, suggesting that in the absence of field MB measurements the geodetic method may be used instead.

Energy balance modelling

Dokriani and Gangotri glaciers are located in close proximity to each other, so experience a similar climate. Since precipitation from the field is not available for Gangotri glacier, precipitation datasets available from the different stations (Tela, Gujjar and base camp) located near Dokriani glacier (30° 49′–30° 52′ N and 78° 47′–78° 51′ E) are used to compare the precipitation data from TRMM, HAR-10, REMO and APHRODITE. Since the field precipitation of Dokriani matches well with the precipitation data from TRMM, HAR-10, REMO and APHRODITE (Fig. 10a), these datasets have also

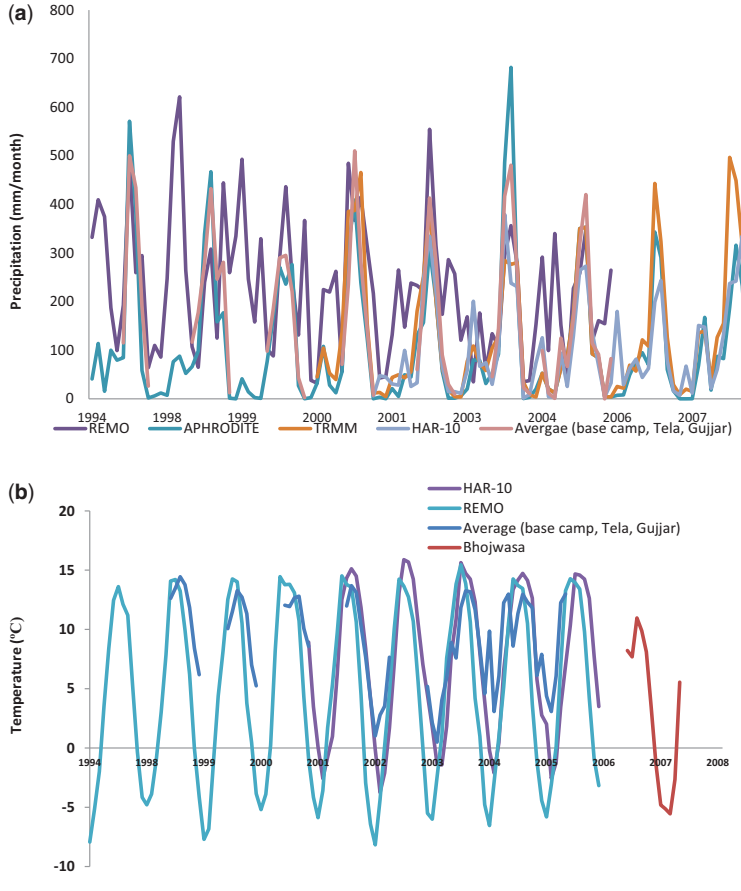

Fig. 10. (**a**) Comparison of temperature datasets acquired from AWS stations (average of Tela, Gujjar hut and base camp and Bhojwasa), REMO and HAR-10 data. (**b**) Comparison of different precipitation datasets (HAR_10, APHRODITE, REMO, TRMM, average of field observations from Tela, Gujjar and base camp of Dokriani glacier).

been used to compute accumulation over Gangotri glacier. However, some parts of the Gangotri glacier are in the monsoon shadow zone; this is reflected in the very low precipitation at Bhojwasa station, averaging *c.* 230 mm a^{-1}. The precipitation distribution at the higher-altitude reaches of the glacier is not known. The model precipitations tally well with the Dokriani catchment stations with heavy precipitation during monsoon months, overwhelming the winter precipitation. Temperature datasets from Tela, Gujjar and base camp are also compared with HAR-10 temperature data at 2 m height from the glacier surface (Fig. 10b). The accumulation in Gangotri glacier MB was measured as 1.509 m w.e. by TRMM, 1.13 m w.e. by APHRODITE and 1.05 m w.e. by HAR-10 for the time period May 2006 to April 2007. Accumulation is estimated by the precipitation in the accumulation zone; accumulation for the period May 2006–April 2007 using TRMM, APHRODITE and HAR-10 datasets is shown in Figure 11a. Net longwave radiation, net shortwave radiation, sensible heat flux, latent heat flux and net radiation are computed for every month (Fig. 11b, Table 4). Melt is computed for one whole year. According to AWS data from Nandanvan station, the melt is 4.4 m w.e. a^{-1}. This gives annual point MB to be −2.891 m w.e. at Nandanvan station, −3.27 m w.e. and −3.35 m w.e. when accumulation is computed from TRMM, APHRODITE and HAR-10 precipitation datasets, respectively.

The mean annual mass balance computed using the method described in 'Mean MB from energy balance modelling using temperature lapse rate' is determined to be −0.53 (precipitation taken from TRMM), −0.63 (precipitation taken from APHRODITE) and −0.65 m w.e. (precipitation taken from HAR-10) when temperatures computed for individual bands of the glaciers are averaged over the entire glacier.

The mean annual mass balance computed using the TLR and albedo parameterization is calculated as −0.82 m w.e., −0.84 m w.e. and −0.92 m w.e. using precipitation data from TRMM, APHRODITE and HAR-10, respectively.

The monthly energy balance fluxes computed are compared with the energy fluxes given for

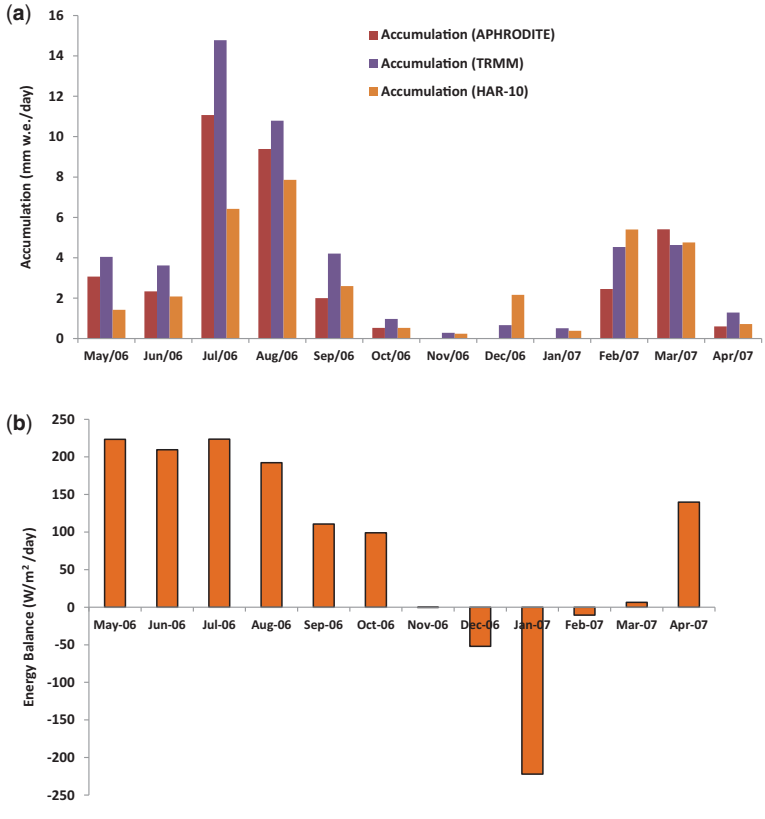

Fig. 11. (**a**) Accumulation over Gangotri glacier estimated using APHRODITE, HAR-10 and TRMM data. (**b**) Energy balance estimated using AWS data.

Table 4. Monthly average energy balance parameters computed using Nandanvan AWS data

	Net SWR (W m^{-2})	Net LWR	Sensible heat flux	Latent heat flux	Net radiation
May 2006	262	−68	16	12	223
June 2006	231	−63	16	26	210
July 2006	212	−44	28	28	224
August 2006	197	−50	22	23	192
September 2006	158	−66	17	2	111
October 2006	210	−93	*c.* 0	−18	99
November 2006	156	−112	−15	−29	*c.* 0
December 2006	130	−117	−23	−43	−52
January 2007	91	−123	−81	−109	−222
February 2007	40	−121	−74	−84	−240
March 2007	64	−112	−58	−89	−195
April 2007	170	−90	4	−58	26

Chhota Shigri glacier, including net shortwave radiation (201 W m^{-2}), net longwave radiation (−-15 W m^{-2}), sensible heat flux (31 W m^{-2}) and latent heat flux (11 W m^{-2}), for the time period 8 July 2013 to 5 September 2013 (Azam *et al.* 2014). Average net shortwave radiation, net longwave radiation, sensible heat flux and latent heat flux over Gangotri glacier for the months of July 2006 and August 2006 are 205, −47, 24.8 and 25 W m^{-2} respectively.

Net longwave radiation, net shortwave radiation and net turbulent heat fluxes estimated using REMO data are observed to vary over the ranges −31 to −107, 40–243 and −127 to 3 W m^{-2},

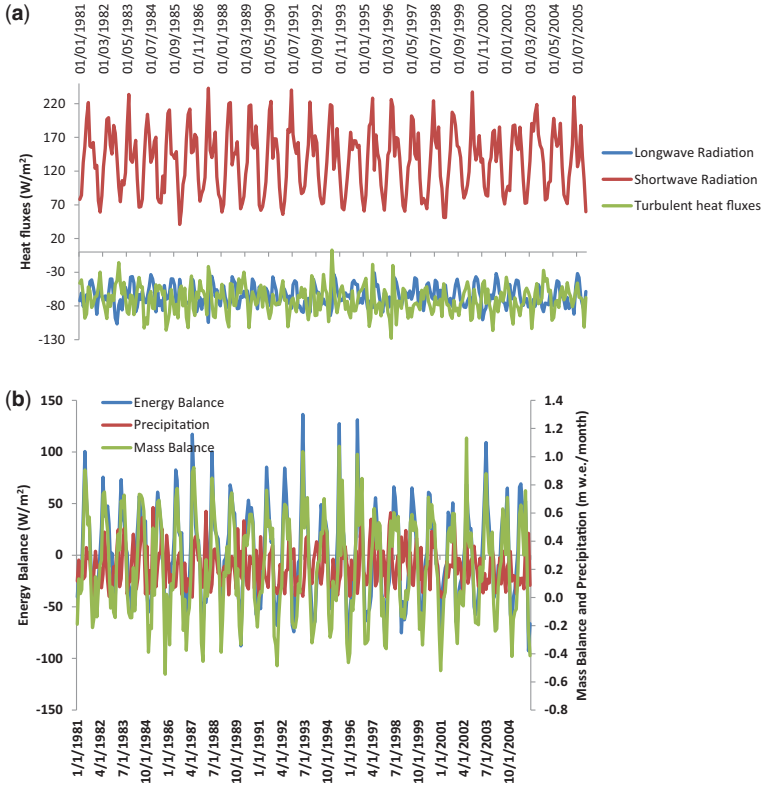

Fig. 12. Monthly (**a**) net longwave radiation, net shortwave radiation and net turbulent heat fluxes and (**b**) MB, precipitation and energy balance estimated using REMO (CORDEX) data.

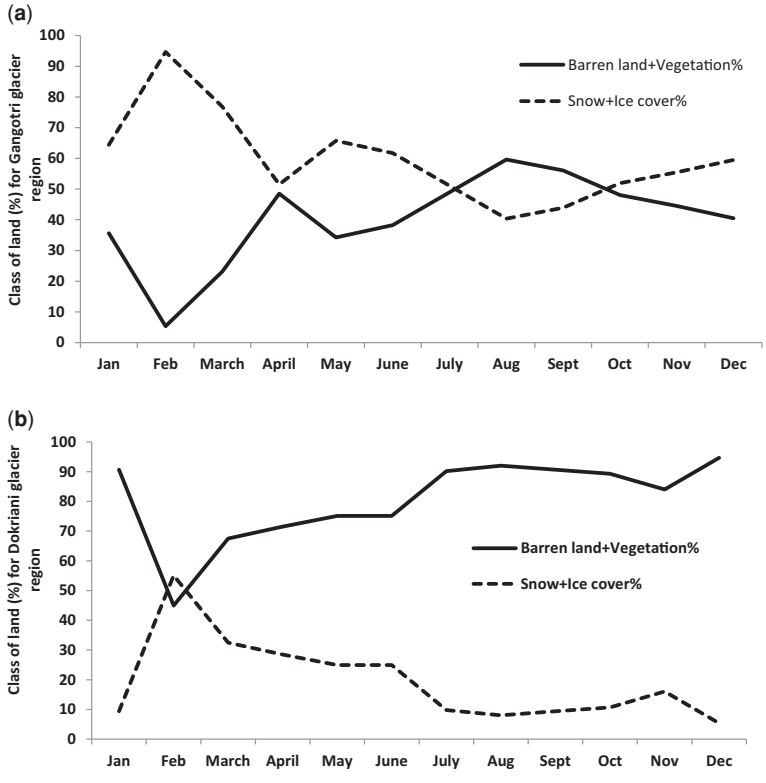

Fig. 13. Percentage of snow+ice cover and vegetation+debris+barren land in REMO grid for (**a**) Gangotri glacier and (**b**) Dokriani glacier.

respectively (Fig. 12a). Precipitation downloaded from the model varies over the range 2–639 mm w.e. per month (Fig. 12b).

The MB computed using REMO data is -0.98 ± 0.23 m w.e. a^{-1} for the time period 1985–2005 (Fig. 12b). Since field MB values are available from Dokriani glacier but not from Gangotri glacier, the MB for Dokriani glacier is also computed using REMO data to compare the closeness in the results of MB computed using REMO data and the field MB values. The REMO data provides a mass balance value of -0.98 m w.e. a^{-1} for the time period 1985–2005, whereas according to Dobhal *et al.* (2008) the glacier's field MB is -0.32 m w.e. a^{-1}

Table 5. *MB computed for Gangotri and Dokriani glaciers using different methods*

Method	Gangotri glacier		Dokriani glacier	
	MB (m w.e. a^{-1})	Time period	MB (m w.e. a^{-1})	Time period
Energy balance modelling (REMO data)	-0.98 ± 0.23	1985–2005	-0.98 ± 0.23	1985–2005
Energy balance modelling (AWS, TRMM data)	-0.82	2006–2007		
Energy balance modelling (AWS, APHRODITE data)	-0.84	2006–2007		
Energy balance modelling (AWS, HAR-10 data)	-0.92	2006–2007		
Geodetic method			-0.27	1995–2008
Ice-flow velocity method	-0.92 ± 0.36	2001–2014		
Field MB			-0.32	1992–2000

for the time period 1992–2000. From Figure 13a, b it is observed that the REMO grid of Dokriani glacier is mostly covered with debris, vegetation and barren land, whereas the REMO grid for Gangotri glacier is mostly covered with snow and ice throughout the year. Due to the small percentage of glacier- and snow-covered areas on Dokriani glacier on the REMO grid, the model is not able to capture the glacier–atmosphere energy balance dynamics accurately and hence the field MB values of Dokriani glacier do not match the MB computed for the glacier using REMO data. However, mass balance estimated for Dokriani glacier by geodetic method during 1995–2008 period (-0.27 m w.e. a^{-1}) is much closer to the field estimation. In the case of Gangotri glacier, the MB computed for the glacier using REMO data is close to the MB computed for the glacier using other methods; that the REMO grid for the Gangotri glacier is therefore able to capture the glacier–atmosphere interaction effectively. This result is indicative of the challenges involved in estimating the glacier-wide weather parameters from climate products, especially for medium- and small-sized glaciers in the Himalaya. Further research is needed to understand the glacier-scale gradients of weather parameters and obtain further improvements in the assessment of climate forcing.

Uncertainty in the area estimate of Gangotri glacier is 1%, dependent upon the resolution of the data used. Uncertainties in the glacier's thickness and volume estimates computed using ice-flow velocity are *c.* 31% and 32%, respectively. The uncertainty in MB computed is estimated as 41%.

The surface velocity method used in this paper depends on the difference in glacier volumes between the years 2001 and 2014. The thickness is calculated with an uncertainty of 30%, which mainly depends on the uncertainty in the values of creep parameter, shape factor and density of ice. The values of these parameters are not expected to change over the period of study, so the volume change calculated by subtraction of volumes is also expected to have 30% error. As also shown by Equation (22), the percentage error of mass balance is given by the sum of errors of thickness and ice density; the error estimate of mass balance is therefore *c.* 40%. The mass balance calculated by the surface velocity method for Gangotri glacier in this study is -0.92 m w.e. a^{-1}, yielding an estimated uncertainty for mass balance of 0.36 m w.e. a^{-1}. This uncertainty is of the order of the uncertainties involved in other methods such as glaciological, geodetic and climatological; Zemp *et al.* (2013) stated that overall mass balance uncertainties are typically about a few hundred millimetres water equivalent per annum, though uncertainties of >0.5 m w.e. a^{-1} have also been reported.

Conclusions

With the help of satellite data, this study has provided a first-order estimate of the MB of Gangotri glacier using different methods. From the analyses, the following insights were obtained.

- Mass balance estimates for Gangotri glacier from different methodologies are remarkably close (Table 5): ice-flow velocity method yielded -0.92 m w.e. a^{-1}; and energy balance modelling yielded -0.82 m w.e. a^{-1} using AWS along with TRMM data and -0.98 m w.e. a^{-1} using REMO data.
- Uncertainty in the area estimate of Gangotri glacier is 1%. Uncertainty in its thickness estimates computed using ice-flow velocity is *c.* 31%. Uncertainty in the volume estimates for the glacier computed using ice-flow velocity method is *c.* 32%. Uncertainty in MB is 41%.
- Gangotri glacier lost around 9% of its volume from 2001 to 2014. This suggests that there is a need to study the regional climatology of the region during the past few decades to understand the reasons for this rapid volume loss of the glacier.
- It has been inferred that the glacier–atmosphere complexities can be further understood by using downscaled data, albedo parameterization and improved knowledge of the relationships between precipitation/temperature and elevation. The results of future studies could be improved by incorporation of these non-linear complexities associated with the glacier–atmosphere dynamic system.

The authors acknowledge the financial assistance received from Science Engineering Research Board (SERB), Department of Science and Technology, under Project No. SB/DGH-50/2013.

References

Ambinakudige, S. 2010. A Study of the Gangotri Glacier Retreat in the Himalayas using Landsat Satellite Images. *International Journal of Geoinformatics*, **6**, 7–12.

Azam, M.F., Wagnon, P., Vincent, C., Ramanathan, A., Linda, A. & Singh, V.B. 2014. Reconstruction of the annual mass balance of Chhota Shigri glacier, Western Himalaya, India, since 1969. *Annals of Glaciology*, **55**, 69–80, https://doi.org/10.3189/2014AoG66A1F04

Berthier, E., Arnaud, Y., Rajesh, K., Sarfaraz, A., Wagnon, P. & Chevallier, P. 2007. Remote sensing estimates of glacier mass balances in Himachal Pradesh (Western Himalaya, India). *Remote Sensing of Environment*, **108**, 327–338.

Bhambri, R., Bolch, T., Chaujar, R.K. & Kulshreshtha, S.C. 2011. Glacier changes in the Garhwal Himalaya,

India, from 1968 to 2006 based on remote sensing. *Journal of Glaciology*, **57**, 543–556.

Bhambri, R., Bolch, T. & Chaujar, R.K. 2012. Frontal recession of Gangotri Glacier. *Current Science*, **102**, 489–494.

Bintanja, R. & van den Broeke, M.R. 1994. Local climate, circulation and surface energy balance of an Antarctic blue ice area. *Annals of Glaciology*, **20**, 160–168.

Bolch, T., Pieczonka, T. & Benn, D.I. 2011. Multi-decadal mass loss of glaciers in the Everest area (Nepal Himalaya) derived from stereo imagery. *The Cryosphere*, **5**, 349–358.

Brock, B.W., Willis, I.C. & Sharp, M.J. 2000. Measurement and parameterization of albedo variations at Haut Glacier d'Arolla, Switzerland. *Journal of Glaciology*, **46**, 675–688.

Cooper, A.P.R., Tate, J.W. & Cook, A.J. 2007. Estimating ice thickness in South Georgia from SRTM elevation data. *International Archives of the Photogrammetry, Remote sensing and Spatial Information Sciences*, **38** (II), 592–597.

Dimri, A.P. 2012. Wintertime Land Surface Characteristics in climatic Simulations over the Western Himalayas. *Journal of Earth System Sciences*, **121**, 329–344.

Dobhal, D.P. & Mehta, M. 2010. Surface morphology, elevation changes and Terminus retreat of Dokriani Glacier, Garhwal Himalaya: implication for climate change. *Himalayan Geology*, **31**, 71–78.

Dobhal, D.P., Gergan, J.T. & Thayyen, R.J. 2008. MB studies of the Dokriani Glacier from 1992-2000, Garhwal Himalaya, India. *Bulletin of Glaciological Research*, **25**, 9–17.

Dobhal, D.P., Mehta, M. & Srivastava, D. 2013. Influence of debris cover on terminus retreat and mass changes of Chorabari Glacier, Garhwal region, central Himalaya, India. *Journal of Glaciology*, **59**, 961–971.

Frey, H., MacHguth, H. *et al.* 2014. Ice volume estimates for the Himalaya–Karakoram region: evaluating different methods. *The Cryosphere*, **8**, 2313–2333.

Gantayat, P., Kulkarni, A.V. & Srinivasan, J. 2014. Estimation of ice thickness using surface velocities and slope: case study at Gangotri glacier, India. *Journal of Glaciology*, **60**(220), 277–282.

Haeberli, W. & Hoelzle, M. 1995. Application of inventory data for estimating characteristics of and regional climate-change effects on mountain glaciers: a pilot study with the European Alps. *Annals of Glaciology*, **21**, 206–212.

Haq, M.A., Jain, K. & Menon, K.P.R. 2013. Volumetric glacier changes in the Garhwal Himalayas using multitemporal digital elevation model, from 2001 to 2010. *35th International Symposium on Remote Sensing of Environment (ISRSE)*, April 22–26, Beijing.

Haq, M.A., Jain, K. & Menon, K.P.R. 2014. Modelling of Gangotri glacier thickness and volume using an artificial neural network. *International Journal of Remote Sensing*, **35**, 6035–6042, http://doi.org/10.1080/01431161.2014.943322

Haritashya, U.K., Singh, P., Kumar, N. & Gupta, R.P. 2006. Suspended sediment from the Gangotri Glacier: Quantification, variability and associations with discharge and air temperature. *Journal of Hydrology*, **321**, 116–130.

Hock, R. 2005. Glacier melt: a review of processes and their modelling. *Progress in Physical Geography*, **29**, 362–391.

IPCC 2007. Climate change 2007: the physical science basis. *Contribution of Working Group I to the Fourth Assessment Report of the Intergovernmental Panel on Climate Change*. Cambridge University Press, Cambridge, United Kingdom and New York, NY, USA.

Kargel, J.S., Cogley, J.G., Leonard, G.J., Haritashya, U. & Byers, A. 2011. Himalayan glaciers: the big picture is a montage. *Proceedings of the National Academy of Science, USA*, **108**, 14709–14710, https://doi.org/10.1073/pnas.1111663108

Kaser, G., Fountain, A. & Jansson, P. 2003. A manual for monitoring the mass balance of mountain glaciers, IHP-VI. Technical Documents in Hydrology, No. 59, UNESCO, Paris.

Kumar, K., Miral, M.S., Joshi, V. & Panda, S. 2002. Discharge and suspended sediment in the meltwater of Gangotri Glacier, Garhwal Himalaya, India. *Hydrological Sciences Journal*, **47**, 611–619.

Kumar, K., Dumka, R.K., Miral, M.S., Satyal, G.S. & Pant, M. 2008. Estimation of retreat rate of Gangotri glacier using rapid static and kinematics GPS survey. *Current Science*, **94**, 258–261.

Kumar, R., Areendran, G. & Rao, P. 2009. *Witnessing Change: Glaciers in the Indian Himalayas*. WWF-India and Birla Institute of Technology, Pilani.

Linsbauer, A., Paul, F. & Haeberli, W. 2012. Modeling glacier thickness and bed topography over entire mountain ranges with GlabTop: Application of a fast and robust approach. *Journal of Geophysical Research*, **117**, 1–17.

Negi, H.S., Thakur, N.K. & Snehmani, A.G. 2012. Monitoring of Gangotri glacier using remote sensing and ground observations. *Journal of Earth System and Sciences*, **121**, 855–886.

Oerlemans, J. 2001. *Glaciers and Climate Change*. Wilco B.V., Netherlands.

Prata, A.J. 1996. A new longwave formula for estimating downward clear-sky radiation at the surface. *Quarterly Journal of the Royal Meteorological Society*, **122**, 1127–1151.

Raina, V.K. 2009. *Himalayan Glaciers: a State-of-Art Review of Glacial Studies, Glacial Retreat and Climate Change*. MoEF Discussion Paper. Ministry of Environment and Forests, Government of India/G.B. Pant Institute of Himalayan Environment and Development, New Delhi/Kosi-Katarmal, Almora.

Saraswat, P., Syed, T.H., Famiglietti, J.S., Fielding, J., Crippen, R. & Gupta, N. 2013. Recent changes in the snout position and surface velocity of Gangotri glacier observed from space. *International Journal of Remote Sensing*, **34**, 8653–8668, http://doi.org/10.1080/01431161.2013.845923

Singh, P., Haritashya, U.K., Ramasastri, K.S. & Kumar, K. 2005. Diurnal variations in discharge and suspended sediment concentration, including runoff-delaying characteristics, of the Gangotri Glacier in the Garhwal Himalayas. *Hydrological Processes*, **19**, 1445–1457.

Singh, P., Haritashaya, U.K. & Kumar, N. 2008. Modelling and estimation of different components of

streamflow for Gangotri Glacier basin, Himalayas. *Hydrological Sciences (Journal des Sciences Hydrologiques)*, **53**, 309–322.

Singh, P., Kumar, A., Kumar, N. & Kishore, N. 2010. Hydro-meteorological correlations and relationships for estimating streamflow for Gangotri Glacier basin in Western Himalayas. *International Journal of Water Resources and Environmental Engineering*, **2**, 60–69.

Thayyen, R.J. 2008. Lower recession rate of Gangotri glacier during 1971–2004. *Current Science*, **95**, 9–10.

Thayyen, R.J. & Gergan, J.T. 2010. Role of glaciers in watershed hydrology: a preliminary study of a Himalayan catchment. *The Cryosphere*, **4**, 115–128.

Yatagai, A., Kamiguchi, K., Arakawa, O., Hamada, A., Yasutomi, N. & Kitoh, A. 2012. APHRODITE: Constructing a long-term daily gridded precipitation dataset for Asia based on a dense network of rain gauges. *American Meteorological Society*, https://doi.org/10.1175/BAMS-D-11-00122.1

Zemp, M., Hoelzle, M. & Haeberli, W. 2009. Six decades of glacier mass-balance observations: a review of the worldwide monitoring network. *Annals of Glaciology*, **50**, 101–111.

Zemp, M., Thibert, E. *et al.* 2013. Reanalysing glacier mass balance measurement series. *The Cryosphere*, **7**, 1227–1245, https://doi.org/10.5194/tc-7-1227-2013